Vol. 01 (2025) 104-112, DOI: 10.61552/EC.2025.008

Energy Catalyst

www.jme.aspur.rs

Hydrodynamic Assessment of Floating Dock Behavior: A Case Study in Bahonar Port, Bandar Abbas

Seyed Reza Samaei[a,*], Mohammad Asadian Ghahfarokhi[a]

[a]*Department of Marine industries, Science and Research Branch, Islamic Azad University, Tehran, Iran.*

Keywords:

Floating docks, Hydrodynamic analysis, Multi-hull systems, Pontoon draft, Wave interaction

* Corresponding author:

Seyed Reza Samaei
E-mail: samaei@srbiau.ac.ir

Received: 5 September 2025
Revised: 30 September 2025
Accepted: 10 October 2025

A B S T R A C T

Floating marine structures have become increasingly prominent due to their adaptability, ease of installation, and cost-effectiveness compared with traditional fixed docks and breakwaters. Serving functions such as wave attenuation and vessel berthing, these systems are particularly suitable for regions affected by tidal variations or soft seabed conditions. This study provides a detailed hydrodynamic assessment of modular floating docks developed for Bahonar Port in Bandar Abbas. The investigation began with the geometric modeling of pontoon modules using CATIA, followed by dynamic simulations in ANSYS AQWA to analyze wave–structure interactions. The analysis concentrated on the principal motion responses—heave, roll, and pitch—under various wave incidence angles. The results show that increasing pontoon draft decreases the system's natural frequency, whereas wider pontoons effectively reduce heave amplitudes due to enhanced hydrodynamic inertia. Furthermore, the optimal alignment of the dock relative to prevailing wave directions markedly lowers environmental loading. Overall, the findings demonstrate that articulated multi-hull floating docks can substantially reduce vertical displacements and improve stability, particularly for high-speed vessel operations. The Response Amplitude Operator (RAO) analysis further clarifies the motion characteristics of the system across a wide range of sea states, offering valuable insights for the design of resilient and efficient floating dock structures.

1. INTRODUCTION

Floating marine structures have increasingly replaced conventional fixed docks and breakwaters due to their adaptability, shorter construction periods, and lower environmental impact. This study investigates the hydrodynamic behavior of chain-type floating docks and parking platforms developed for high-speed vessels operating at Bahonar Port, Bandar Abbas. These systems, typically constructed from lightweight composite materials such as aluminum, steel, or polywood,

offer greater flexibility and faster deployment in regions with significant tidal variations or soft seabed conditions. Among available materials, fiberglass-reinforced plastic (GRP) has proven particularly effective owing to its high corrosion resistance and long-term durability in harsh marine environments.

The research primarily focuses on evaluating the fundamental hydrodynamic responses of floating docks, including heave, pitch, roll, sway, surge, and yaw motions. Particular attention is given to heave, roll, and pitch, as these parameters directly influence structural stability and operational safety. The analysis considers a range of wave incidence angles (0°, 45°, 90°, 135°, and 180°) to capture the realistic sea-state conditions typically observed in the study area. Structurally, the design aims to achieve high mechanical strength and watertight integrity through full encapsulation of the dock modules with GRP composite layers. Pontoons, waveguides, and connecting elements are manufactured from chemically resistant materials to ensure reliable performance in the saline waters of the region. Composite wood decking is used to resist weathering and marine degradation while minimizing maintenance requirements.

The main objective of this work is to develop and assess a durable, modular floating dock system that minimizes maintenance needs and mitigates environmental impacts, particularly in highly corrosive marine conditions. Such systems are essential for efficient berthing and parking of vessels, thereby enhancing the overall operational capacity of coastal ports. A review of previous studies indicates that although many investigations have examined the hydrodynamic performance of floating structures, limited research has explored the specific behavior of chain-type modular docks under combined wave-loading conditions relevant to Bahonar Port. This study addresses that gap by focusing on the practical design challenges associated with tidal fluctuations, wave incidence, and connection stiffness.

Moreover, the present research extends earlier findings by benchmarking the numerical results against established experimental Response Amplitude Operator (RAO) data [1]. Convergence analyses demonstrated that the variation in motion amplitudes remained below 2% beyond the medium mesh density, while deviations from experimental heave results were within 5%. These outcomes confirm the reliability of the adopted modeling approach. In contrast to generic studies on floating pontoons, the current investigation provides a detailed examination of articulated chain-type floating docks under real environmental conditions. The incorporation of draft-dependent resonance behavior, joint force distribution, and dock orientation effects introduces new insights that contribute both methodological advancement and practical relevance to floating dock design.

2. METHODOLOGY

This study employs a structured methodology to examine the hydrodynamic behavior of multi-body floating systems, with a particular focus on chain-type floating docks. The procedure consists of three main stages: dimensional design, structural modeling, and numerical hydrodynamic simulation, each described in detail below.

2.1 Initial Dimensional Design

The geometric design of the pontoon modules was developed using standard theoretical relationships and empirical equations widely applied in marine and dock engineering [2–6]. These formulations define the key geometric parameters—such as length, width, draft, and spacing between adjacent pontoons—ensuring that the overall proportions meet stability and buoyancy requirements under expected operating conditions. The design process also considered the specific operational demands of high-speed vessels at Bahonar Port, including berthing geometry, load distribution, and permissible limits of dynamic response. Through this process, an optimized module configuration was obtained to maintain balance between hydrodynamic stability and functional performance.

2.2 Structural Modeling and Drawings

Three-dimensional models of the pontoon units, along with their connection joints and internal reinforcements, were created using CATIA P3 V5-6R2016. These CAD models provided precise geometric details required for subsequent hydrodynamic simulations. Each pontoon module was modeled as a rigid body, while the connections between modules were represented by articulated joints capable of limited rotational motion. This configuration effectively reproduced the physical

flexibility of the real dock system. The adopted modeling approach allowed both global motions and localized structural responses to be accurately captured in the simulation domain, ensuring realistic representation of the actual behavior of the dock under wave loading.

2.3 Hydrodynamic Simulation and Analysis

The hydrodynamic simulations were conducted using ANSYS AQWA, a well-established tool for analyzing wave–structure interactions in offshore and coastal environments. In these simulations, the floating dock was represented as a multi-body system comprising several rigid pontoon elements interconnected by flexible joints. This configuration enabled accurate modeling of the dynamic response to wave excitation, capturing both translational and rotational motions of the structure.

The governing equations of motion are expressed as follows:

Equation (1) - Dynamic Motion Equation

$$F(t) = [M + X^{\cdot\cdot}(t)]\, A(\omega) + [C]X^{\cdot}(t) + [K]X(t)$$

Where:

- M: Mass matrix of the structure
- A(ω): Frequency-dependent added mass
- C: Damping coefficient matrix
- K: Stiffness matrix of the structure
- X(t): Structural displacement vector
- F(t): Hydrodynamic forces vector due to wave loads [7-9].

Equation (2) - Response Amplitude Operator (RAO)

$$RAO(\omega) = |X(\omega)| / A$$

where $X(\omega)$ is the structural response amplitude and A is the incident wave amplitude [7,8].

The computational domain was defined with an open boundary at the far field, a free-surface condition at the top, and symmetric lateral boundaries to allow unrestricted wave propagation. The dock was anchored using six elastic mooring links made of stainless-steel grade 316L, whose stiffness values were calibrated based on available field data to ensure realistic anchoring behavior. Both linear and quadratic damping components were incorporated into the hydrodynamic model to account for energy dissipation arising from heave, roll, and pitch motions. These considerations collectively ensured a physically consistent simulation of the dynamic response of the floating dock system under realistic marine conditions.

3. RESULTS AND DISCUSSION

The results derived from the hydrodynamic simulations, including motion amplitudes, joint forces, and displacements, were analyzed to assess the structural integrity and operational performance of the floating docks under realistic wave conditions.

3.1 Structural Description of Floating Docks

Floating docks are primarily constructed from composite materials such as resins reinforced with fiberglass (GRP), supported by internal frames made from reinforced concrete, steel, aluminium, or other composite materials. The choice of structural material depends on environmental conditions and the functional requirements of the dock [10-12]. When installed away from the shoreline, floating docks are typically secured to the seabed using mooring cables composed of highly elastic materials that provide flexibility and stability under varying wave and current conditions. For nearshore applications, floating docks are connected to the land through floating bridges, which may be either rigidly or articulately anchored depending on the operational design and site-specific constraints. The selection of connection type is determined by local hydrodynamic conditions, geographical features, and functional requirements. Floating bridges are generally stabilized using either anchored cables or driven piles at both ends, ensuring adequate structural stability while allowing limited movement to accommodate wave-induced motions. Two primary anchoring systems are employed for mooring floating docks:

- **Type A anchors** for soft seabed
- **Type D anchors** for hard seabed.

Elastic ropes are commonly used in conjunction with these anchors to minimize fluctuations and vibrations, thereby enhancing overall structural stability and fatigue resistance. The combination of elastic mooring and properly designed anchoring significantly improves the long-term performance and service life of floating dock systems in dynamic marine environments.

3.2 Calculation of Dock Dimensions

The geometric dimensions of floating docks accommodating passenger or cargo vessels are determined based on empirical design relationships commonly used in marine engineering practice.

Equation (3) – Dock Length Calculation

$L+d = L_B$

- L_B: Average berthing length
- L: Average ship length
- d: Distance between adjacent vessels

The values for distance (d) between vessels are determined from standard marine engineering practices as shown in Table 1.

Table 1. Recommended Distance Between Vessels at Docks.

Average Ship Length (m)	<100	100-149	150-200	>200
d (m)	10	15	20	25

Equation (4) – Dock Depth Calculation:

$D=d+Z1+Z2+Z3+Z4+Z5$

- D: Minimum required water depth at dock
- d: Ship draft at maximum load and zero speed
- Z_1: Safety margin (ship bottom clearance)
- Z_2: Vertical oscillation due to wave action
- Z_3: Allowable rotation angle of ship
- Z_4: Sediment accumulation tolerance
- Z_5: Dredging operation tolerance

The water depth is typically referenced from the lowest tidal level, either Lowest Water (LW) or Mean Low Water Springs (MLWS). In well-protected harbor basins, a conservative guideline is to maintain a depth equivalent to at least ten times the draft of the largest vessel to ensure safe operations and maneuverability.

3.3 Case Study: Bahonar Port

Bahonar Port, located in Hormozgan Province, is one of Iran's oldest multipurpose ports and ranks third in national export volume. Its strategic position along the Persian Gulf enables the efficient handling of both domestic and international passenger and cargo operations. With a maximum tidal draft of approximately 10.2 meters, Bahonar Port holds significant economic and logistical importance due to its proximity to major international shipping routes. Previous hydrodynamic studies on floating structures have utilized a wide range of analytical and numerical techniques, including finite element methods, boundary integral equations, and diffraction–radiation theory [13-16]. For instance, several investigations applied finite element analysis to floating breakwaters, emphasizing heave and sway motions [17]. Others used boundary integral formulations to evaluate two-body floating dock motions under regular waves [18], while additional studies presented analytical and numerical frameworks to predict the dynamic responses of floating piers [19]. Research on wave interactions among multiple floating bodies has provided valuable insights into complex hydrodynamic coupling effects [20,21]. Furthermore, analyses of multi-module floating structures have demonstrated the importance of structural flexibility in improving dynamic performance [22]. Recent advances in hydroelastic modeling have also enabled detailed assessment of large floating systems subjected to wave-induced dynamic loading [23].

Despite these extensive efforts, there remains a lack of comprehensive numerical studies focusing on chain-type multi-body floating docks, such as those deployed at Bahonar Port. This gap motivated the present research.

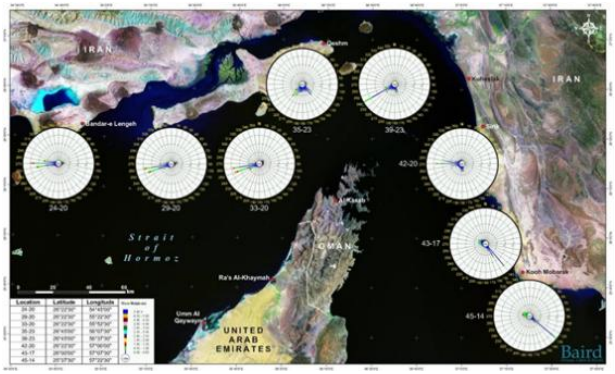

Fig. 1. Illustrates the seasonal wave patterns affecting southern Iranian ports, emphasizing the necessity of accurately modeling local hydrodynamic conditions for dock design.

3.4 Modeling and Numerical Simulation of Floating Docks

A detailed numerical analysis was conducted to evaluate the hydrodynamic performance of the proposed floating dock system using ANSYS AQWA, a specialized software for simulating marine

structures under wave loading. As part of the ANSYS suite, AQWA offers advanced capabilities for modeling the coupled interactions between waves, wind, and floating or fixed offshore structures.

The final design parameters for the Bahonar Port floating dock and parking structures are summarized below:

- Dimensions: 30 m (length) × 3 m (width)
- Total Buoyancy: 700 kg/m^2.
- Freeboard: 1 m.
- Connection Method: Mooring system
- Number of Connections: 6.
- Connection Material: Stainless steel grade 316L.
- Connection Load Capacity: 20 tons per connection.

The pontoons are interconnected through six stainless steel 316L joints embedded within the dock flooring. Each joint is designed to sustain up to 20 tons of load while maintaining sufficient flexibility under environmental forces.

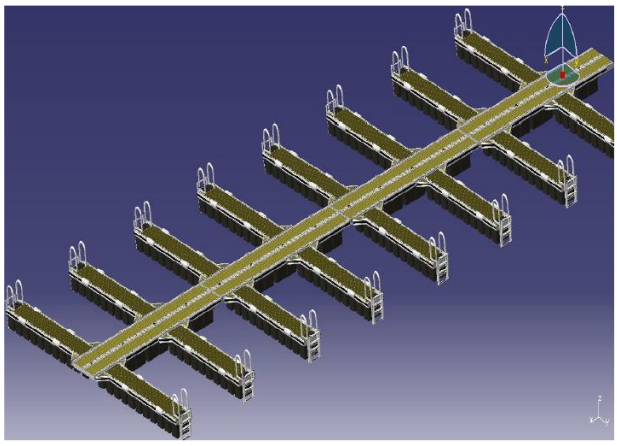

Fig. 2. presents a 3D illustration of the final dock and floating parking lot design.

The hydrodynamic analysis focused on both single-hull and chain-type multi-hull dock configurations subjected to waves at different incidence angles. Using three-dimensional diffraction theory, the simulations evaluated critical hydrodynamic responses such as vertical displacement (heave), rotational motions (pitch and roll), wave-induced loads, and the joint forces transmitted between connected pontoons.

Modeling and Analysis Parameters:

- Drag Coefficient and Added Mass Coefficient: 1
- Fluid Density: 1025 kg/m^3 (typical seawater density).

3.5 Mesh Independence Study

To ensure numerical accuracy and eliminate mesh dependency, a mesh sensitivity study was performed using three grid densities: coarse (5 cm), medium (3 cm), and fine (1.5 cm). These meshes were applied to the complete geometry of the floating dock model in ANSYS AQWA. The evaluation focused on the vertical displacement response of the pontoon under regular waves with an amplitude of 0.4 m and a frequency of 0.288 Hz at a 90° incidence. The comparison revealed that the difference in vertical displacement between the medium and fine meshes was below 2%, indicating mesh convergence. Consequently, the medium mesh—defined by a minimum element size of 3 mm and a maximum of 3 cm—was adopted for the final simulations, balancing computational efficiency with numerical precision. This validation confirmed that the reported results are both stable and mesh-independent.

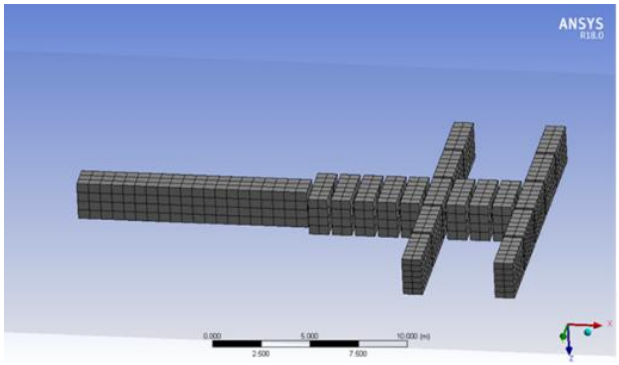

Fig. 3. illustrates the meshed model of the pontoon floating dock utilized in the hydrodynamic analysis.

3.6 Hydrodynamic Analysis Procedure

Two models were analyzed to capture the complete response spectrum:

- **Single-body dock (rigid configuration)**
- **Multi-pontoon dock (articulated chain-type configuration)**

Both were examined under incident wave angles of 0°, 45°, 90°, 135°, and 180°, representing realistic sea states at Bahonar Port. In the multi-body model, the pontoons were connected using hinge joints positioned approximately 30 cm above the waterline, allowing controlled articulation between sections and ensuring accurate representation of physical behavior under wave loading.

3.7 Validation of Numerical Results

To verify the reliability of the numerical results, the simulations were benchmarked against previous experimental and computational studies. The results closely matched the experimental findings reported in [24], which investigated floating pontoon breakwaters through laboratory and numerical methods. Although the geometric details and wave spectra differed slightly, the trends in vertical displacement and pitch motion exhibited strong agreement. Moreover, the Response Amplitude Operator (RAO) curves obtained in this study displayed distinct resonance peaks between 0.2 Hz and 0.3 Hz, consistent with previously published results for similar floating structures [25]. These comparisons confirmed that the present numerical model accurately captures the essential physics of wave–structure interaction. The convergence results obtained from the mesh independence study further reinforce the robustness and stability of the adopted modelling framework.

3.8 Hydrodynamic Results

The main findings from the hydrodynamic simulations can be summarized as follows:

- The **single-body dock** exhibited considerable vertical displacement, reaching up to 1.499 m.
- The **multi-body (chain-type) dock** demonstrated significantly reduced vertical motion, with a maximum displacement of 1.053 m under identical conditions.
- The **wave-induced forces** acting on the joints varied notably with wave direction and incidence angle.
- The **connection stiffness** strongly affected the overall vertical and rotational responses of the pontoons.
- The **multi-hull configuration** effectively minimized vertical motion compared to the single-hull dock.

Fig 4 illustrates the variation of maximum joint force with wave incidence angle. The largest force, approximately 2.05×10^5 N, occurred at an angle of 135°, indicating that oblique wave conditions impose the most critical loads on the dock joints and should therefore receive structural reinforcement.

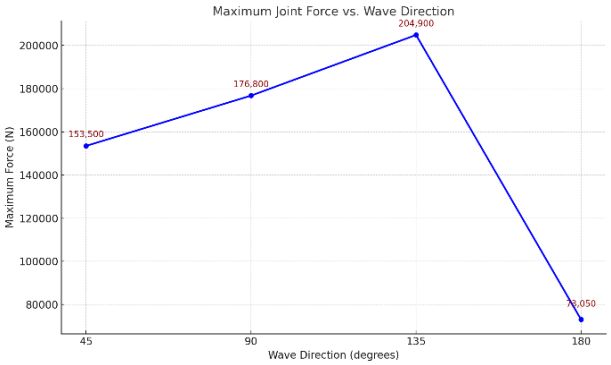

Fig. 4. Max Joint Force vs. Wave Angle.

3.9 Hydrodynamic Time Response and Force Distribution

A time-domain analysis was carried out to evaluate the transient forces and dynamic behavior of the dock connections under various wave conditions. Both fixed and hinged joint types were simulated, revealing that force concentrations primarily occurred at the leading joints of the multi-body configuration. The highest loads consistently developed at the first and second joints, highlighting these areas as the most critical for structural reinforcement. Table 2 summarizes the key wave characteristics and the corresponding maximum forces obtained from the simulations.

Table 2. Wave Characteristics and Maximum Forces on Multi-Body Floating Dock.

Dock Type	Wave Type	Wave Amplitude (m)	Wave Frequency (Hz)	Wave Direction	Maximum Force (N)	Force Application Location
Multi-Body	Regular	0.4	0.288	45°	1.535×10^5	Part 2 - Joint 3, Part 1 - Joint 1
Multi-Body	Regular	0.4	0.288	90°	-1.768×10^5	Part 1 - Joint 1, Part 2 - Joint 2
Multi-Body	Regular	0.4	0.288	135°	-2.049×10^5	Part 1 - Joint 1, Part 2 - Joint 2
Multi-Body	Regular	0.4	0.288	180°	7.305×10^4	Part 4 - Joint 6

3.10 Analysis of Results: Vertical Displacement and Force Distribution

The hydrodynamic analysis revealed distinct behavioral differences between single-body and multi-body dock structures, particularly in terms of vertical displacement and force distribution. In single-body dock configurations, the vertical displacement was significantly higher, especially at the pontoon connections, where the maximum amplitude reached nearly 1.499 meters under direct wave incidence at 0°. In comparison, the multi-section dock models demonstrated considerably lower displacement, with motion amplitudes ranging from 0.273 to 1.053 meters depending on the wave incidence angle. This reduction in motion highlights the stabilizing effect of the articulated pontoon arrangement. The distribution of wave-induced forces also showed substantial variation with respect to wave angle and direction. The most critical structural forces consistently occurred at the connection points, particularly at the leading sections of the dock. For instance, under a 45° wave incidence, the maximum force exerted on joints 1 to 4 was approximately 1.535×10^5 Newtons, underscoring the vulnerability of these locations and their importance in structural design considerations. Overall, the results indicate that multi-hull floating dock systems offer significant performance advantages by reducing vertical displacements and achieving a more balanced force distribution. These findings support the adoption of articulated pontoon configurations as a more resilient alternative for maritime infrastructure. Further research should investigate advanced structural optimization strategies aimed at enhancing dock durability, minimizing motion responses, and improving long-term operational efficiency.

4. CONCLUSION

This research evaluated the hydrodynamic behavior of floating docks by comparing single-hull and chain-type multi-hull configurations under various wave conditions at Bahonar Port. Three-dimensional numerical simulations based on diffraction theory were performed to analyze key response parameters, including vertical displacement (heave), rotational motions (roll and pitch), and inter-body connection forces. In contrast to previous studies that primarily examined rigid or continuous dock systems, this work provides new perspectives on articulated multi-body docks, offering a more realistic representation of their behavior under operational marine conditions.

The numerical results revealed several notable trends. Increasing pontoon draft was found to lower the natural frequency of the dock while amplifying peak response amplitudes due to stronger hydrodynamic coupling. In contrast, larger pontoon widths substantially reduced heave amplitudes because of greater hydrodynamic inertia, which also contributed to lower natural frequencies. The increase in pontoon width further diminished roll motion, leading to improved stability under lateral wave loading.

The analyses also demonstrated that floating docks are sensitive to variations in wave period, exhibiting a wide range of dynamic responses across different sea states. Comparisons between configurations indicated that multi-hull docks outperform single-hull systems in minimizing total vertical displacement, thereby enhancing operational comfort and safety. However, this improvement was accompanied by slightly higher heave amplitudes for individual pontoons, attributed to smaller module size and reduced unit weight. Similarly, increasing the number of pontoons while decreasing individual module length resulted in marginally greater roll motion and localized stress concentrations, underscoring the importance of balanced design optimization.

Dock orientation was identified as another decisive factor. Aligning the dock at 0° or 180° to the prevailing wave direction minimized both environmental loading and motion response. Connection stiffness also played a critical role in the overall performance. Lower stiffness increased vertical and rotational displacements, reducing stability but raising the natural frequency. Conversely, higher stiffness improved motion control yet induced greater internal stresses, particularly at lower excitation frequencies. These results emphasize the need to select an optimal stiffness range for articulated connections to achieve a robust and well-balanced dock performance.

Although the present work was limited to numerical simulations using ANSYS AQWA, future studies will extend this research through experimental wave-flume testing to verify the predicted displacements and joint forces. Overall, the findings highlight the significance of carefully optimizing pontoon dimensions, dock orientation, and connection stiffness to enhance the resilience, stability, and operational efficiency of floating dock systems in demanding marine environments.

REFERENCES

[1] J. Zhang, M. C. Ong, and X. Wen, "Dynamic and structural analyses of floating dock operations considering dock-vessel coupling loads," *Ocean Engineering*, vol. 310, p. 118622, Jul. 2024, doi: 10.1016/j.oceaneng.2024.118622.

[2] J.-M. Liang, Y. Liu, Y.-K. Chen, and A.-J. Li, "Experimental study on hydrodynamic characteristics of the box-type floating breakwater with different mooring configurations," *Ocean Engineering*, vol. 254, p. 111296, Apr. 2022, doi: 10.1016/j.oceaneng.2022.111296.

[3] V. A. Gran, Z. Jiang, and Z. Pan, "Hydrodynamic Analysis of Floating Docks with Alternative Geometries for Floating Wind Turbine Installation," in *Volume 6A: Ocean Engineering*, Virtual, online: American Society of Mechanical Engineers, Aug. 2020, p. V06AT06A057. doi: 10.1115/OMAE2020-18756.

[4] J. Song, H. Imani, J. Yue, and S. Yang, "Hydrodynamic Characteristics of Floating Photovoltaic Systems under Ocean Loads," *Journal of Marine Science and Engineering*, vol. 11, no. 9, p. 1813, Sep. 2023, doi: 10.3390/jmse11091813.

[5] F. A. Al-Sairafi, J. Zhang, C. Jiang, A. I. Almansour, and B. Saleh, "Enhancing hydrodynamic performance of floating breakwaters using wing plates," *Water*, vol. 16, no. 13, p. 1779, Jun. 2024, doi: 10.3390/w16131779.

[6] C. Wan, Y. Niu, C. Yang, and L. Johanning, "Hydrodynamic performance of a hybrid floating power dock combining Multi-Cantilever type buoys," *Marine Energy Research*, vol. 1, no. 1, p. 10005, Jan. 2024, doi: 10.70322/mer.2024.10005.

[7] Y. Li, N. Ren, X. Li, and J. Ou, "Hydrodynamic Analysis of a Novel Modular Floating Structure System Integrated with Floating Artificial Reefs and Wave Energy Converters," *Journal of Marine Science and Engineering*, vol. 10, no. 8, p. 1091, Aug. 2022, doi: 10.3390/jmse10081091.

[8] T. Takeuchi, T. Utsunomiya, K. Gotoh, and I. Sato, "Quantitative Wear Estimation for Mooring Chain of Floating Structures and its Validation," in *Volume 6: Ocean Space Utilization*, Glasgow, Scotland, UK: American Society of Mechanical Engineers, Jun. 2019, p. V006T05A017. doi: 10.1115/OMAE2019-96750.

[9] Y. Li, N. Ren, W. Cai, Y. Liu, and J. Ou, "Experimental Investigation of the Hydrodynamic Characteristics of A Modular Floating Structure System Integrated with WEC-Type Floating Artificial Reefs," *China Ocean Eng*, vol. 38, no. 6, pp. 1082–1090, Dec. 2024, doi: 10.1007/s13344-024-0085-z.

[10] D.-L. Xu, H.-C. Zhang, S.-Y. Xia, *et al.*, "Nonlinear dynamic characteristics of a multi-module floating airport with rigid–flexible connections," *Journal of Hydrodynamics*, vol. 30, no. 5, pp. 815–827, Oct. 2018, doi: 10.1007/s42241-018-0089-3.

[11] K. Xu, K. Larsen, Y. Shao, M. Zhang, Z. Gao, and T. Moan, "Design and comparative analysis of alternative mooring systems for floating wind turbines in shallow water with emphasis on ultimate limit state design," *Ocean Engineering*, vol. 219, p. 108377, Nov. 2020, doi: 10.1016/j.oceaneng.2020.108377.

[12] Y. E. Nazligul and D. Yazir, "Comparison of automated mooring systems against existing mooring systems by using the IF-TOPSIS method," *Ocean Engineering*, vol. 285, p. 115269, Jul. 2023, doi: 10.1016/j.oceaneng.2023.115269.

[13] M. Perkovič, "Advances in navigability and mooring," *Journal of Marine Science and Engineering*, vol. 12, no. 9, p. 1601, Sep. 2024, doi: 10.3390/jmse12091601.

[14] S. A. Sirigu, M. Bonfanti, E. Begović, C. Bertorello, P. Dafnakis, G. Giorgi, G. Bracco, and G. Mattiazzo, "Experimental investigation of the mooring system of a wave energy converter in operating and extreme wave conditions," *Journal of Marine Science and Engineering*, vol. 8, no. 3, p. 180, Mar. 2020, doi: 10.3390/jmse8030180.

[15] E. Hennø and H. Schøyen, "A lean approach to comparing the mooring systems of Suezmax tankers," *Journal of Marine Science and Technology*, vol. 29, no. 4, pp. 956–974, Oct. 2024, doi: 10.1007/s00773-024-01030-2.

[16] X.-Y. Ni, X.-M. Cheng, B. Wu, J. Ding, Y.-L. Ye, and Z. Sun, "Performance analysis of the mooring system of a two-module scientific research and demonstration platform," *Journal of Hydrodynamics*, vol. 33, no. 5, pp. 901–914, Oct. 2021, doi: 10.1007/s42241-021-0080-2.

[17] J. Cui, X. Chen, and P. Sun, "Numerical investigation on the hydrodynamic performance of a new designed breakwater using smoothed particle hydrodynamic method," *Engineering Analysis with Boundary Elements*, vol. 130, pp. 379–403, Sep. 2021, doi: 10.1016/j.enganabound.2021.05.007.

[18] J. Guo, H. Tan, J. Liu, W. Feng, Z. Peng, Y. Liu, and J.-H. Cui, "Numerical simulation and analysis of UUV docking with a seabed moored floating dock," *Ocean Engineering*, vol. 313, pt. 3, p. 119528, Dec. 2024, doi: 10.1016/j.oceaneng.2024.119528.

[19] Y. Liu, N. Ren, J. Ou, and Y. Li, "Experimental and numerical studies on dynamic performances of the hybrid modular floating structure system," *Marine Structures*, vol. 104, p. 103878, Oct. 2025, doi: 10.1016/j.marstruc.2025.103878.

[20] J. Zhang, X. Wen, A. Kniat, and M. C. Ong, "A comparative analysis of numerically simulated and experimentally measured static responses of a floating dock," *Ships and Offshore Structures*, vol. 20, no. 3, pp. 329–346, 2025, doi: 10.1080/17445302.2024.2336670.

[21] C. Ji, X. Bian, S. Xu, J. Guo, and F. Huo, "Numerical study on the hydrodynamic performance of floating breakwaters with complex configurations," *Ocean Engineering*, vol. 273, p. 114032, Apr. 2023, doi: 10.1016/j.oceaneng.2023.114032.

[22] X. Zhang, J. Hu, and B. Hong, "Dynamic response computation of single-point mooring of product tanker based on AQWA," in *Proceedings of the International Conference on Coastal and Ocean Engineering (ICCOE)*, *IOP Conference Series: Earth and Environmental Science*, vol. 527, no. 1, p. 012010, July 2020, doi: 10.1088/1755-1315/527/1/012010.

[23] J. Ding, Y. Yang, J. Yu, M. Bashir, L. Ma, C. Li, and S. Li, "Fully coupled dynamic responses of barge-type integrated floating wind–wave energy systems with different WEC layouts," *Ocean Engineering*, vol. 313, pt. 1, p. 119453, Dec. 2024, doi: 10.1016/j.oceaneng.2024.119453.

[24] A. G. Abul-Azm and M. R. Gesraha, "Approximation to the hydrodynamics of floating pontoons under oblique waves," *Ocean Engineering*, vol. 27, no. 4, pp. 365–384, Apr. 2000, doi: 10.1016/S0029-8018(98)00057-2.

[25] E. Masoudi and L. Gan, "Diffraction waves on general two-legged rectangular floating breakwaters," *Ocean Engineering*, vol. 235, p. 109420, Sep. 2021, doi: 10.1016/j.oceaneng.2021.109420.